Original paper

Crystal chemistry and evolution of tourmaline in tourmalinites from Zlatá Idka, Slovakia

Peter BAČÍK[1,2,*], Daniel OZDÍN[1], Pavel UHER[1], Martin CHOVAN[1]

[1] *Comenius University in Bratislava, Faculty of Natural Sciences, Department of Mineralogy, Petrology and Economic Geology, Ilkovičova 6, 842 15 Bratislava, Slovak Republic; peter.bacik@uniba.sk*
[2] *Earth Science Institute of the Slovak Academy of Sciences, Dúbravská cesta 9, 840 05 Bratislava, Slovak Republic*
[*] *Corresponding author*

Tourmalinites occur in early-Paleozoic metamorphic rocks of the Gemeric Unit near Zlatá Idka village, Western Carpathians, eastern Slovakia. Tourmaline compositions, analyzed with the electron microprobe, include a wide range of tourmaline species. Tourmaline in tourmalinites from Zlatá Idka is compositionally variable, with the dominant substitution $Mg–Fe^{2+}$ consistent with prevalent schorl–dravite compositions and their fluor- and oxy-dominant counterparts – fluor-schorl, fluor-dravite, oxy-schorl and oxy-dravite. Portions of tourmaline are enriched in Ca in the form of the fluor-uvite and magnesio-lucchesiite components. A subset of the compositions has Ti > 0.25 atoms per formula unit (*apfu*) and corresponds to the hypothetical "magnesio-dutrowite", Mg-dominant analogue of dutrowite. In addition, some of the tourmalines are *X*-site vacant and classified as foitite. The crystal chemistry of tourmaline is complex and influenced by several exchange mechanisms, including $Mg(Fe)_{-1}$, $Al□(Mg,Fe)_{-1}Na_{-1}$, $AlO(Mg,Fe)_{-1}(OH)_{-1}$ $(Mg,Fe)CaAl_{-1}Na_{-1}$, $MgCaOAl_{-1}□_{-1}(OH)_{-1}$, $Ti_{0.5}O(Fe,Mg)_{-0.5}(OH)_{-1}$ and $TiMg(Al)_{-2}$ substitutions. In general, tourmalines in all samples usually have oscillatory-zoned dravitic cores and schorlitic rims (Tur I). However, in ZLT-4 and ZLT-6 samples, some crystals have secondary Mg-dominant and Ca-enriched overgrowths (Tur II), partially replacing Tur I. Tourmalinites were most likely produced by regional or contact metasomatic processes, likely due to the intrusion of the Permian Poproč granitic massif. Origin of tourmalinites likely results from the flow of late-magmatic to early post-magmatic B,F-rich fluids from the granite intrusion into adjacent metamorphic rocks. The tourmaline crystallization and its resulting chemical composition were controlled by both the metapelitic host rock and the granitic intrusion; the Mg-rich cores of the Tur I are most likely compositionally related to the metapelitic host rock, whereas later schorlitic to foititic compositions in rims suggest origin due to the intrusion-triggered fluid flow. The significant changes and oscillations of tourmaline zoning imply a dynamic, unstable fluid regime. The late Ca-rich Tur II could result from subsequent metasomatic processes associated with the alteration of host-rock minerals.

Keywords: tourmaline supergroup, tourmalinites, magnesio-lucchesiite, titanium, metasomatism
Received: 16 December 2021; accepted: 8 August 2022; handling editor: Ferdinando Bosi
The online version of this article (doi: 10.3190/jgeosci.350) contains supplementary electronic material.

1. Introduction

Tourmalinites are defined as rocks that contain over 15 or 20 vol. % of tourmaline (Nicholson 1980; Slack 1982). The dominant minerals of tourmalinites include quartz and tourmaline-supergroup minerals, but commonly they also contain feldspars, mica, chlorite, apatite, and other minerals. Tourmalinites occur over a range of ages, Archean to Phanerozoic, often with base-metal or other ore mineralizations. Tourmalinites are frequently associated with clastic metasedimentary rocks, most commonly metapelitic sequences, but they can also be associated with felsic and/or mafic metavolcanic rocks, occurring preferentially on the contacts between felsic and mafic units, or between either of these and various clastic metasediments (Slack 1996). In addition, some tourmalinites are developed in marine or non-marine meta-evaporites (Behr et al. 1983; Chown 1987; Peng and Palmer 1995; Henry et al. 2008). The metamorphic grade of tourmalinites and their host rocks is usually greenschist or amphibolite, although some tourmalinites are known in metamorphic rocks of zeolite (Zhang et al. 1994) or granulite facies (Slack et al. 1993). Tectonic settings of tourmalinite-bearing sequences vary widely but are mostly connected with rift-related extensional regimes.

Tourmalinites are found at several occurrences in the Western Carpathians, Slovakia. These can be divided into redeposited and *in situ* occurrences. The redeposited West-Carpathian tourmalinites occur as clastic rock fragments in conglomerate horizons within psammitic quartzites of the Lúžna Formation (Upper Permian? to Lower Triassic). These redeposited tourmalinites occur only in the southwestern part of the Tatric Unit in proportions that decrease from the southwest (Malé Karpaty Mountains) to the northeast (Považský Inovec, Tribeč and Strážovské Mountains) (Mišík and Jablonský 2000; Bačík and Uher 2007; Bačík et al. 2008). Rare tourmalinites are

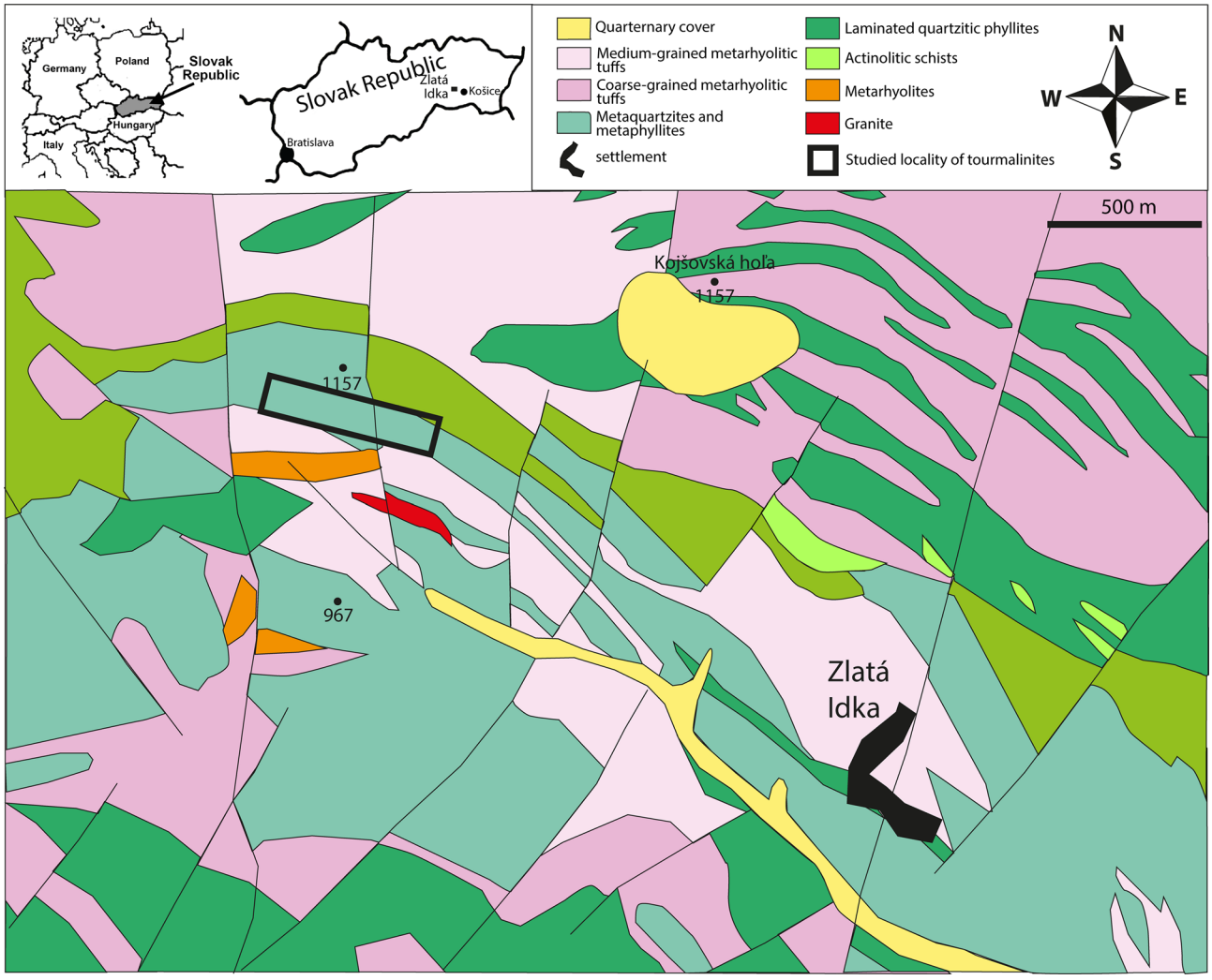

Fig. 1 Geological sketch map of the studied locality (Geological map of Slovakia M 1 : 50 000, modified).

also found as pebbles in the Albian to Cenomanian polymictic conglomerates of the Klape Unit in the Pieniny Klippen Belt, Western Carpathians (Bačík et al. 2008).

In situ occurrences of Western-Carpathian tourmalinites are located in the Paleozoic metamorphosed volcano-sedimentary Jánov Grúň Complex in the Kráľova Hoľa Zone of the Veporic Unit. They likely formed from prograde metamorphism of B-enriched volcano-sedimentary horizons (Bačík et al. 2009). However, the largest and the richest Western-Carpathian occurrence of tourmalinites is located within Paleozoic metamorphic rocks of Gemeric Unit near Zlatá Idka village (Eastern Slovakia). It was explored as a possible tourmaline deposit for use in special radiation-shielding concretes (Navesňák and Tabák 1994; Kobulský et al. 2000; Chovan et al. 2003), but only preliminary microprobe analyses of tourmaline were mentioned in the unpublished report (Chovan et al. 2003). Consequently, the goal of our contribution is a detailed electron-probe (EPMA) study of the chemical composition, zoning and compositional evolution of tourmaline-supergroup minerals in the Zlatá Idka tourmalinites. We discuss the most likely scenarios of the rock origin and factors controlling tourmaline compositional heterogeneity.

2. Geological settings

The Gemeric Unit has a range of tourmaline occurrences, including mostly schorlitic magmatic tourmaline in Permian granitic rocks (Kubiš et al. 2012; Broska and Kubiš 2018) to hydrothermal tourmaline of more variable schorlitic–dravitic composition in siderite-quartz-sulfide (Bačík et al. 2018) and Sb hydrothermal veins (Klimko et al. 2009; Bačík et al. 2017). Moreover, oxy-schorl species was described as a new mineral from metasomatically altered metarhyolite pyroclastics at Zlatá Idka (Bačík et al. 2013).

The Zlatá Idka tourmalinite deposit is located in the Gemeric Unit in Eastern Slovakia (Fig. 1). It is situated

in the exocontact zone of the Permian granitic massif that intruded the Paleozoic (Upper Ordovician to Devonian) metamorphic rocks the Gelnica Group of the Gemeric Unit (Bajaník et al. 1983; Kobulský et al. 2000). The following rock types and tourmaline occurrences were defined here (Kobulský et al. 2000).

(i) Fine- to coarse-grained two-mica to muscovite leucogranites, locally with aplite and quartz-tourmaline dikes (≤ 5 cm in thickness).

(ii) Volcano-sedimentary, medium-grade feldspar-bearing metamorphic rocks (gneisses) near the intrusive contact with the granites. Tourmaline content in this rock does not exceed 1 vol. %.

(iii) Various types of phyllites, quartzites and metarhyolite tuffs with tuffites ("porphyroids"). These metamorphic rocks are significantly enriched in tourmaline, especially quartzites and chloritic–sericitic phyllites with tourmaline-rich metaquartzite to metapsamite layers (tourmalinites). Tourmaline forms within veinlets and laminae, forming distinct tourmalinization zones. The thickness of the tourmalinite formation is from 100 to 150 m; the volume of the whole formation is, therefore, sufficient to meet the parameters for the deposit of tourmaline as a raw material.

Tourmalinites are dark gray rocks with a banded structure formed by alternating layers (thickness of several mm to cm) of pale quartz and dark minerals dominated by tourmaline (up to 75 vol. %); they have heteroblastic to granoblastic texture (Navesňák and Tabák 1994; Chovan et al. 2003). The dominant minerals in the tourmalinites are quartz and tourmaline; the average content of acicular tourmaline attains 42.8 vol. %, equivalent to ~4.3 wt. % B_2O_3 for the whole rock (Navesňák and Tabák 1994). Potassic feldspar, albite, chlorite, mica, fluorite, sulfides, and secondary iron oxides and hydroxides are accessory phases (Kobulský et al. 2000; Chovan et al. 2003).

3. Analytical methods

The seven studied samples are representative of specific lithotypes of tourmalinites in the Zlatá Idka deposit; thin sections were prepared of the samples ZLT-1 through ZLT-3 (two from each) and ZLT-4 through ZLT-7 (one from each).

The chemical composition of tourmaline was obtained with a CAMECA SX100 electron microprobe in WDS mode at the State Geological Institute of Dionýz Štúr, Bratislava, using the following analytical conditions: accelerating voltage 15 kV, beam current 20 nA, beam diameter 2 to 5 μm. The following standards were used

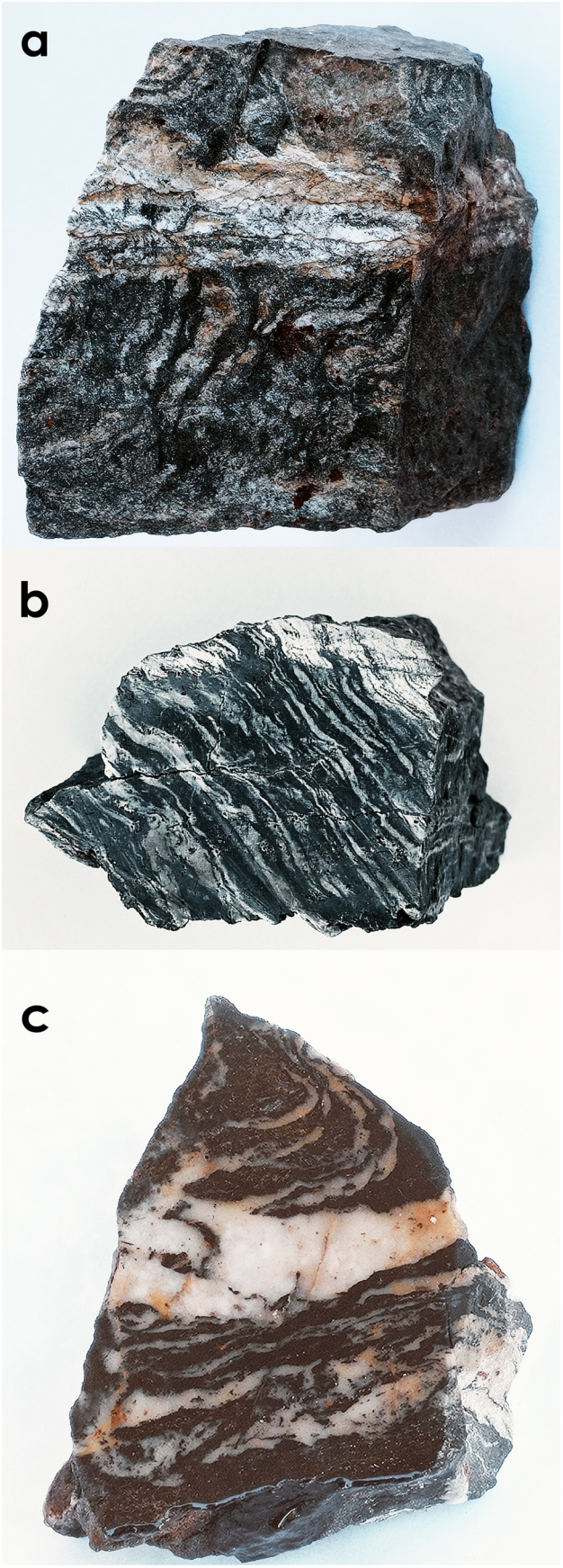

Fig. 2 Studied samples of tourmalinites from Zlatá Idka. **a** – ZLT-2 sample (size 30 × 54 mm). **b** – (b) ZLT-4 sample (75 × 58 mm). **c** – ZLT-6 sample (62 × 68 mm).

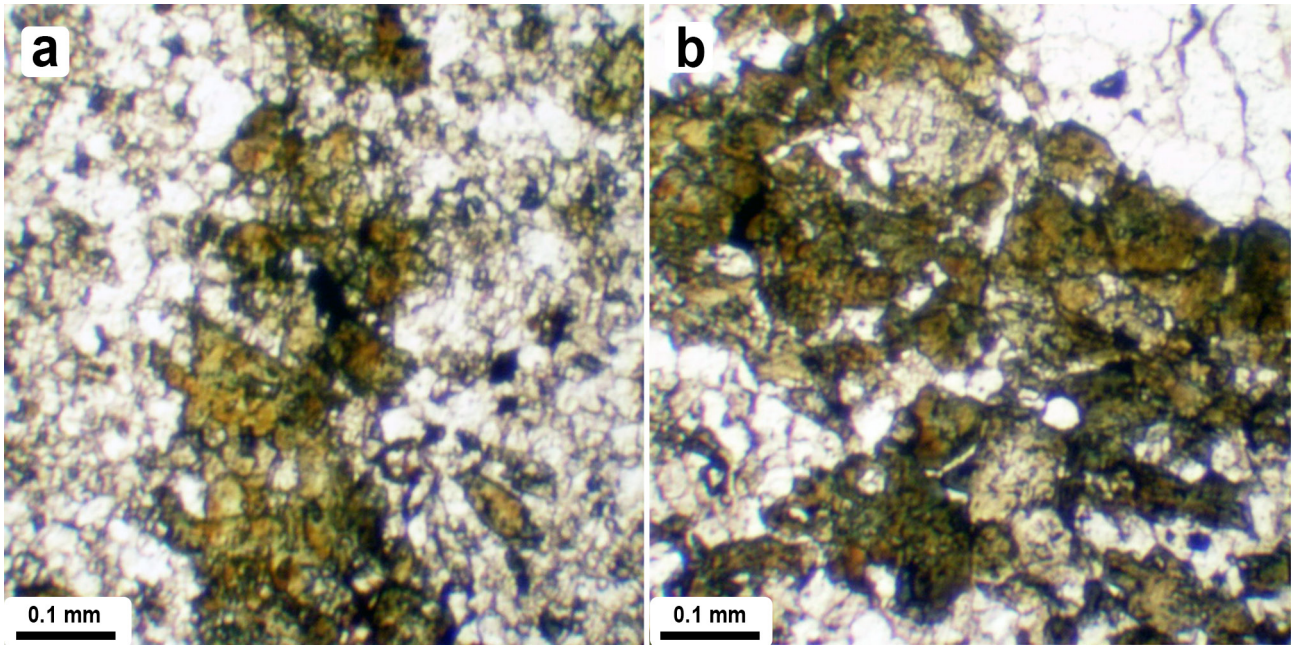

Fig. 3 Microphotographs of tourmalinites from Zlatá Idka in parallel nicols: **a** – ZLT-1A; **b** –ZLT-3A sample.

(all measured on K_α spectral lines): wollastonite (Si, Ca), TiO_2 (Ti), Al_2O_3 (Al), chromite (Cr), metallic V (V), hematite (Fe), rhodonite (Mn), MgO (MgK_α), willemite (ZnK_α), metallic Ni (NiK_α), albite (NaK_α), orthoclase (KK_α), BaF_2 (FK_α), and NaCl (ClK_α). Matrix corrections were done using the "*PAP*" routine. The detection limits of the microprobe for the measured elements were in the range 0.01–0.05 wt. %, and the accuracy varied between 0.1 to 0.5 wt. % at optimal conditions. The chemical formulae of tourmalines were calculated on the basis of 15 $Y+Z+T$ cations, B_2O_3 was calculated assuming 3.00 B *apfu*; when applicable, O^{2-} was calculated to match the charge-balanced formula. Water contents were calculated assuming $^{V,W}(OH+O+F+Cl)=4$ *apfu*.

4. Results

4.1. Mineral association

Samples ZLT-1 to ZLT-7 are dark grey rocks with a heteroblastic to granoblastic and layered texture consisting of alternating light- and dark-colored bands (Fig. 2). Light bands consist of quartz ± albite and muscovite, dark bands are dominated by tourmaline with minor biotite, chlorite, sulfides (pyrite, arsenopyrite ± chalcopyrite), and Fe-oxides and hydroxides. The light to dark minerals ratio is approximately 60 : 40. Occasional brown Fe-oxides and hydroxides coatings are caused by the release of iron from altered mafic minerals, especially pyrite. The ZLT-7 sample has thicker light-colored layers, with the total ratio of quartz to dark-colored minerals being approximately 70 : 30. The macroscopic appearance of the rocks ranges from schists to tourmalinized metaquartzites.

Tourmaline forms prismatic crystals up to ~500 μm long and ~10−70 μm thick; individual crystals are euhedral to subhedral, except for sections parallel to the *c* axis. Tourmaline is pleochroic from light brown to green (Fig. 3). The sections perpendicular to the *c* axis have characteristic zoning represented by two distinct types of zones – a darker brown to the green core, and a paler green rim (Fig. 3).

Accessory minerals of the tourmalinites include monazite-(Ce), xenotime-(Y), fluorapatite, zircon, rutile, ilmenite, and unspecified (U,Th)–(Nb,Ta) oxide mineral identified by EDS.

4.2. Tourmaline chemical composition and zoning

Most tourmaline analyses belong to the alkali group, but calcic and *X*-site vacant tourmalines are also present (Tabs 1, 2; Fig. 4a). Occupancy of the *W*-site shows a large compositional variability; the analyzed tourmalines are almost evenly distributed among the hydroxy-, fluor-, and oxy-tourmalines (Fig. 4b). The most common compositions belong to schorlitic and dravitic tourmalines, however, some are also foititic (Fig. 5a) and uvitic (Fig. 5c).

Tourmaline from Zlatá Idka has a distinct optical and chemical zoning. Tourmaline crystals developed in several stages. The individual zones often have very contrasting chemistry. In general, tourmalines in all samples have dravitic cores and schorlitic rims (Tur I) (Fig. 4), but the ZLT-4 and ZLT-6 samples have, in addition, Mg-

dominant and Ca-enriched rims (Tur II) which overgrow and discontinuously replace more ferrous tourmaline cores (Tur I; Figs 4e, f). The Tur I crystal cores usually display oscillatory zoning; the composition heterogeneity varies among the individual samples (Figs 2b–e). The largest compositional variation between tourmaline cores and rims was observed in the ZLT-3 sample, where the Fe/(Fe+Mg) ratio varies from 0.2 in the dravitic cores to 0.5 to 0.9 in the schorlitic rims (Figs 6a, b). The majority of Fe is likely ferrous, as indicated by the good correlation between Fe and Mg (Fig. S1a, ESM1); however, in the ZLT-3 and ZLT-4 samples, part of Fe is likely ferric as it relatively significantly correlates with Al (Fig. S1b, ESM2). The *X*-site vacancy usually increases from the dravitic core (< 0.2 *pfu*) to the schorlitic rim zones (> 0.3 *pfu*), even attaining foitite composition in the ZLT-1 and ZLT-7 samples (Figs 6a, 7). On the other hand, the *X*-site vacancy decreases to less than 0.1 *pfu* in the ZLT-4 and ZLT-6 samples with Ca-rich Tur II.

Tourmalines have an extremely variable distribution of $(OH)^-$, F^- and O^{2-} anions at the *W* site (Fig. 5b), but no general correlation is visible within or among the samples. Fluorine preferentially concentrates in Mg-rich (dravite to fluor-dravite) compositions in ZLT-1, ZLT-2 and ZLT-4 samples, although F-rich schorl to fluor-schorl compositions are also present. In the ZLT-6 sample, F prefers schorlitic compositions. The concentration of $^{W}O^{2-}$ increases with Al, preferentially producing oxy-dravite in ZLT-1–4 samples and also oxy-schorl in ZLT-3 and ZLT-6 samples.

Tab. 1 Representative electron-microprobe analyses of tourmaline from ZLT-1–3 samples (in wt. % and *apfu*).

	ZLT-1 Fdrv	ZLT-1 Foi	ZLT-1 Osrl	ZLT-2 Odrv	ZLT-2 Srl	ZLT-2 "Mdtw"	ZLT-3 Odrv	ZLT-3 Fsrl	ZLT-3 Ti Srl
SiO_2	37.19	36.18	37.37	37.80	36.70	36.01	37.69	36.10	34.88
TiO_2	0.59	0.30	0.20	0.27	1.45	3.09	0.26	1.66	1.94
B_2O_3*	10.74	10.47	10.75	10.83	10.35	10.58	10.84	10.47	10.08
Al_2O_3	31.05	35.05	35.64	35.29	29.12	32.42	35.77	31.09	27.89
Cr_2O_3	0.00	0.00	0.01	0.06	0.02	0.17	0.00	0.07	0.00
V_2O_3	0.03	0.05	0.00	0.00	0.00	0.13	0.03	0.05	0.01
FeO	7.13	12.24	8.53	6.52	12.81	8.32	4.15	12.02	17.93
MnO	0.01	0.06	0.02	0.01	0.00	0.02	0.00	0.07	0.00
MgO	8.31	1.50	4.09	5.59	4.35	5.05	6.70	4.08	1.86
NiO	0.04	0.00	0.00	0.01	0.02	0.00	0.00	0.05	0.00
ZnO	0.07	0.10	0.00	0.00	0.00	0.03	0.00	0.09	0.02
CaO	0.34	0.03	0.14	0.31	0.41	0.24	0.10	0.30	0.56
Na_2O	2.62	1.43	1.88	1.87	2.36	1.97	1.85	2.23	2.20
K_2O	0.03	0.03	0.04	0.04	0.05	0.04	0.02	0.04	0.07
H_2O*	3.08	3.06	3.10	3.11	3.05	2.98	3.18	2.71	3.16
F	1.22	0.33	0.17	0.16	0.38	0.19	0.13	1.29	0.37
Cl	0.00	0.01	0.00	0.01	0.01	0.01	0.00	0.00	0.02
O=F	0.51	0.14	0.07	0.07	0.16	0.08	0.05	0.54	0.16
O=Cl	0.00	0.00	0.00	0.00	0.00	0.00	0.00	0.00	0.00
Total	101.94	100.70	101.87	101.81	100.92	101.16	100.66	101.78	100.83
Si^{4+}	6.018	6.007	6.042	6.068	6.162	5.916	6.045	5.991	6.014
$Al^{3+}T$	0.000	0.000	0.000	0.000	0.000	0.084	0.000	0.009	0.000
∑T	6.018	6.007	6.042	6.068	6.162	6.000	6.045	6.000	6.014
B^{3+}	3.000	3.000	3.000	3.000	3.000	3.000	3.000	3.000	3.000
$Al^{3+}Z$	5.922	5.993	5.999	5.992	5.762	5.962	5.996	5.984	5.667
Cr^{3+}	0.000	0.000	0.001	0.008	0.003	0.021	0.000	0.009	0.000
V^{3+}	0.004	0.007	0.000	0.000	0.000	0.017	0.004	0.007	0.001
Mg^{2+}	0.074	0.000	0.000	0.000	0.235	0.000	0.000	0.000	0.331
∑Z	6.000	6.000	6.000	6.000	6.000	6.000	6.000	6.000	6.000
Ti^{4+}	0.072	0.037	0.024	0.033	0.183	0.382	0.031	0.207	0.252
Al^{3+}	0.000	0.865	0.792	0.684	0.000	0.231	0.765	0.087	0.000
Fe^{2+}	0.965	1.699	1.153	0.875	1.799	1.143	0.557	1.668	2.585
Mn^{2+}	0.001	0.008	0.003	0.001	0.000	0.003	0.000	0.010	0.000
Mg^{2+}	1.930	0.371	0.986	1.338	0.854	1.237	1.602	1.009	0.147
Zn^{2+}	0.008	0.012	0.000	0.000	0.000	0.004	0.000	0.011	0.003
Ni^{2+}	0.005	0.000	0.000	0.001	0.003	0.000	0.000	0.007	0.000
∑Y	2.982	2.993	2.958	2.932	2.838	3.000	2.955	3.000	2.986
Ca^{2+}	0.059	0.005	0.024	0.053	0.074	0.042	0.017	0.053	0.103
Na^+	0.822	0.460	0.589	0.582	0.768	0.629	0.575	0.718	0.735
K^+	0.006	0.006	0.008	0.008	0.011	0.008	0.004	0.008	0.015
$^{X}\square$	0.113	0.528	0.378	0.356	0.147	0.321	0.403	0.221	0.146
∑X	0.887	0.472	0.622	0.644	0.853	0.679	0.597	0.779	0.854
F^-	0.624	0.173	0.087	0.081	0.202	0.096	0.066	0.677	0.202
Cl^-	0.000	0.003	0.000	0.003	0.003	0.003	0.000	0.000	0.006
O^{2-}	0.051	0.430	0.570	0.581	0.381	0.633	0.531	0.325	0.157
OH^-	3.000	3.000	3.000	3.000	3.000	3.000	3.000	2.998	3.000
OH^-	0.325	0.394	0.343	0.335	0.414	0.267	0.403	0.000	0.635
∑*V*+*W*	4.000	4.000	4.000	4.000	4.000	4.000	4.000	4.000	4.000

*calculated

Interestingly, tourmalines from Zlatá Idka tourmalinites commonly display a significant enrichment in Ti. All samples contain zones with Ti above 0.1 *apfu* (Fig. 6c) with a maximum of 0.38 *apfu* (3.09 wt. % TiO_2, Tab. 1). The Ti contents increase in two distinct

Tab. 2 Representative electron-microprobe analyses of tourmaline from ZLT-4–7 samples (in wt. % and *apfu*).

	ZLT-4 Fdrv	ZLT-4 Srl	ZLT-4 Fluvt	ZLT-6 Fsrl	ZLT-6 Mlcc	ZLT-7 Drv	ZLT-7 Srl	ZLT-7 Osrl	ZLT-7 Foi
SiO_2	37.81	36.15	37.25	36.60	37.01	37.89	36.57	37.35	37.58
TiO_2	0.33	0.04	0.53	0.81	1.14	0.43	0.84	0.38	0.25
B_2O_3*	10.83	10.35	10.71	10.37	10.53	10.72	10.42	10.75	10.73
Al_2O_3	30.95	32.21	28.49	30.78	28.57	32.08	30.86	35.06	35.14
Cr_2O_3	0.06	0.00	0.01	0.01	0.01	0.01	0.04	0.01	0.00
V_2O_3	0.06	0.05	0.03	0.05	0.28	0.02	0.07	0.05	0.02
FeO	3.06	15.07	4.52	12.38	4.65	4.12	11.29	8.38	9.23
MnO	0.02	0.05	0.00	0.02	0.01	0.01	0.04	0.04	0.02
MgO	10.88	1.67	11.67	3.71	10.20	8.69	4.55	4.49	3.83
NiO	0.00	0.00	0.00	0.00	0.00	0.01	0.02	0.00	0.00
ZnO	0.01	0.00	0.00	0.02	0.02	0.08	0.01	0.07	0.00
CaO	1.40	0.08	3.39	0.24	2.80	0.28	0.30	0.08	0.06
Na_2O	1.95	1.88	1.18	2.31	1.41	2.08	2.02	1.85	1.30
K_2O	0.02	0.02	0.04	0.03	0.02	0.03	0.03	0.04	0.02
H_2O*	3.11	3.06	2.95	2.80	3.09	3.19	3.03	3.21	3.31
F	0.95	0.73	1.12	0.85	0.10	0.52	0.71	0.13	0.11
Cl	0.00	0.01	0.01	0.01	0.01	0.00	0.01	0.00	0.00
O=F	0.40	0.31	0.47	0.36	0.04	0.22	0.30	0.05	0.05
O=Cl	0.00	0.00	0.00	0.00	0.00	0.00	0.00	0.00	0.00
Total	101.04	101.06	101.42	100.64	99.81	99.94	100.51	101.84	101.56
Si^{4+}	6.070	6.071	6.045	6.137	6.107	6.143	6.099	6.038	6.085
$\mathbf{Al^{3+}}\boldsymbol{T}$	0.000	0.000	0.000	0.000	0.000	0.000	0.000	0.000	0.000
∑T	6.070	6.071	6.045	6.137	6.107	6.143	6.099	6.038	6.085
B^{3+}	3.000	3.000	3.000	3.000	3.000	3.000	3.000	3.000	3.000
$\mathbf{Al^{3+}}\boldsymbol{Z}$	5.856	5.993	5.449	5.991	5.557	5.996	5.985	5.992	5.997
Cr^{3+}	0.008	0.000	0.001	0.002	0.002	0.001	0.005	0.001	0.000
V^{3+}	0.008	0.007	0.004	0.007	0.037	0.003	0.009	0.006	0.003
Mg^{2+}	0.129	0.000	0.546	0.000	0.404	0.000	0.000	0.000	0.000
∑Z	6.000	6.000	6.000	6.000	6.000	6.000	6.000	6.000	6.000
Ti^{4+}	0.040	0.005	0.065	0.102	0.141	0.052	0.105	0.046	0.030
Al^{3+}	0.000	0.382	0.000	0.091	0.000	0.134	0.080	0.687	0.708
Fe^{2+}	0.411	2.117	0.613	1.736	0.641	0.559	1.575	1.133	1.250
Mn^{2+}	0.003	0.007	0.000	0.003	0.001	0.001	0.006	0.005	0.003
Mg^{2+}	2.475	0.418	2.277	0.928	2.106	2.100	1.131	1.082	0.924
Zn^{2+}	0.001	0.000	0.000	0.002	0.003	0.010	0.001	0.008	0.000
Ni^{2+}	0.000	0.000	0.000	0.000	0.000	0.001	0.003	0.000	0.000
∑Y	2.930	2.929	2.955	2.863	2.893	2.857	2.901	2.962	2.915
Ca^{2+}	0.241	0.014	0.589	0.043	0.495	0.049	0.054	0.014	0.010
Na^{+}	0.607	0.612	0.371	0.750	0.450	0.654	0.653	0.580	0.408
K^{+}	0.004	0.004	0.008	0.007	0.004	0.006	0.006	0.008	0.004
$^{X}\square$	0.148	0.369	0.031	0.200	0.051	0.291	0.287	0.398	0.577
∑X	0.852	0.631	0.969	0.800	0.949	0.709	0.713	0.602	0.423
F^{-}	0.482	0.388	0.575	0.453	0.052	0.267	0.374	0.066	0.056
Cl^{-}	0.000	0.003	0.003	0.002	0.003	0.000	0.003	0.000	0.000
O^{2-}	0.184	0.180	0.231	0.413	0.538	0.281	0.255	0.471	0.371
OH^{-}	3.000	3.000	3.000	3.000	3.000	3.000	3.000	3.000	3.000
OH^{-}	0.334	0.430	0.191	0.131	0.407	0.452	0.367	0.463	0.573
∑*V*+*W*	4.000	4.000	4.000	4.000	4.000	4.000	4.000	4.000	4.000

*calculated

compositional trends (Fig. 6c): (1) Fe-dominant tourmaline in the schorl–dutrowite trend – mostly in ZLT-1–4 samples; (2) Mg-dominant tourmaline in the dravite–"magnesio-dutrowite" trend in the ZLT-2 and ZLT-6 samples. Compositions with Ti > 0.25 *apfu* in the ZLT-2 and ZLT-3 samples could be classified as "magnesio-dutrowite" and dutrowite, respectively. Since dutrowite is oxy-tourmaline, only compositions in the ZLT-2 sample with calculated ^{W}O > 0.5 apfu and $^{Y}Ti > {}^{Y}Al$ could be classified as a potentially new tourmaline-supergroup mineral "magnesio-dutrowite". The Ti-rich compositions from ZLT-3 sample have the calculated ^{W}O below 0.5 *apfu*. Although it is possible that ^{W}O may be underestimated due to the possible presence of Fe^{3+}, it is more likely that the increased Ti contents in the samples are charge-balanced by the substitution of Mg for Al at the neighboring *Z* site. Therefore, although Ti is slightly above 0.25 *apfu* here, it does not satisfy the dutrowite composition.

The crystal rims (Tur II) in the ZLT-4 and ZLT 6 samples display significant enrichment in Ca, which locally becomes the dominant *X*-site cation. In the ZLT-4 sample, Ca exceeds 0.50 *apfu* resulting in fluor-uvite. In the ZLT-6 sample, the Ca-dominant and Mg-dominant tourmaline with $^{VI}Al > 5.5$ *apfu* and calculated $^{W}O > 0.5$ *apfu* has a magnesio-lucchesiite composition (Fig. 6d, Tab. 2).

Compositional trends revealed that the complex composition of studied tourmalines results from various substitutions. The direction of the Al-increase vector compared to the *X*-site vacancy and the near-linear array of the more aluminous samples indicate that it is charge-balanced by both $Al\square(Mg,Fe)_{-1}Na_{-1}$ and $AlO(Mg,Fe)_{-1}(OH)_{-1}$ substitutions (Fig. 8a). However, low-Al compositions manifest the importance of $(Mg,Fe)CaAl_{-1}Na_{-1}$

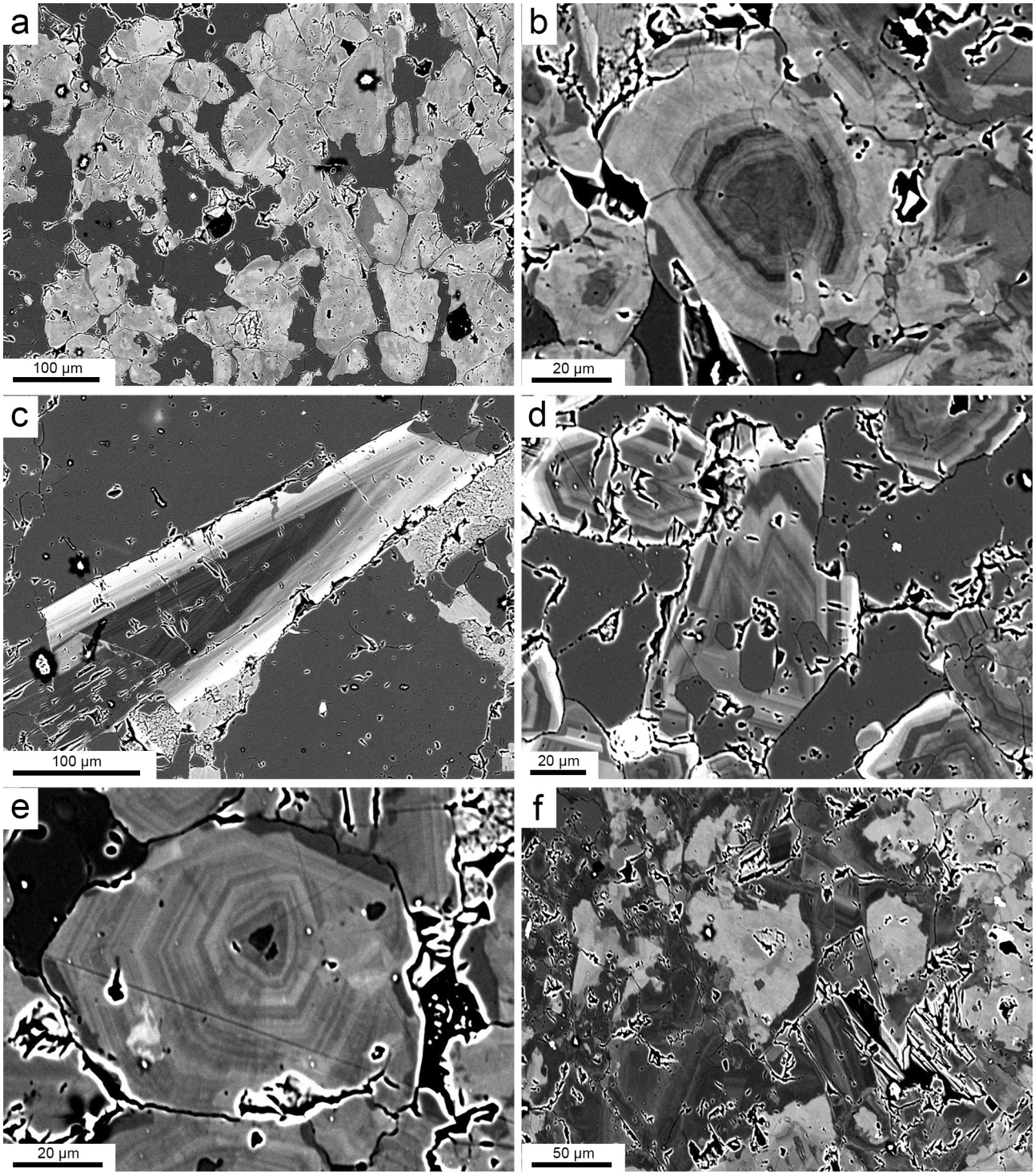

Fig. 4 Back-scattered electron images of tourmalinites from Zlatá Idka. **a** – ZLT-1 sample; **b** – ZLT-2 sample; **c, d** –ZLT-3 sample; **e** – ZLT-4 sample; **f** – ZLT-7 sample.

substitution (Fig. 8b). The division of compositions into two groups with different substitutional mechanisms is clearly visible when individual substitutions (Figs 9a, b) or their combinations (Fig. 9c) are examined; Ca-dominant compositions separated from the majority of analyses. The enrichment in Ca is clearly controlled by $(Mg,Fe)CaAl_{-1}Na_{-1}$ (Fig. 9a) or the combined (Mg,Fe) $CaOAl_{-1}Na_{-1}(OH)_{-1}$ (Fig. 9c) exchange, while the $Al\square(Mg,Fe)_{-1}Na_{-1}$ substitution (Fig. 9b) shows no correlation in these compositions. Increased Ti could result from $Ti_{0.5}O(Fe,Mg)_{-0.5}(OH)_{-1}$ substitution ("magnesiodutrowite") or $TiMg(Al)_{-2}$ (Al-depleted Ti-enriched com-

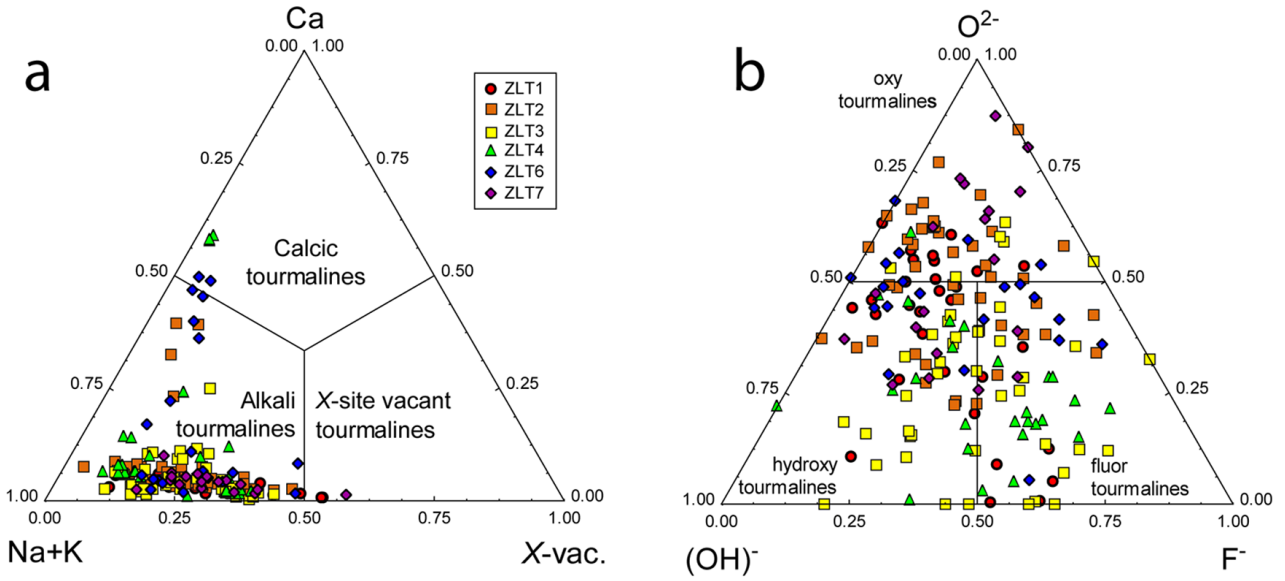

Fig. 5 Toumaline classification. **a** – calcic, alkali and *X*-site vacant subgroups. **b** – hydroxy-, fluor- and oxy- series.

positions) substitution, although Ti can be involved in even more complex substitutions.

5. Discussion

5.1. Mineral composition and crystal chemistry of tourmalinites

Tourmaline in tourmalinites from Zlatá Idka displays a large compositional variability. Along with the common schorl–dravite composition, their fluor- and oxy-dominant counterparts – fluor-schorl, fluor-dravite, oxy-schorl and oxy-dravite – are also present. Moreover, portions of the tourmaline are enriched in Ca resulting in fluor-uvite and magnesio-lucchesiite, which is tourmaline derived from uvite with O^{2-} dominant at the *W* site and the sum of trivalent cations at *Z* above 5.5 *apfu* (Scribner et al. 2021). Moreover, the areas with Ti-rich compositions having Ti > 0.25 *apfu* likely correspond to a potential new mineral species, "magnesio-dutrowite", which would be the Mg-dominant analog of dutrowite (Biagioni et al. 2020). Finally, the *X*-vacant tourmaline is foitite. Consequently, the crystal chemistry of tourmaline at this locality is complex and influenced by several substitution mechanisms.

The simplest octahedral $FeMg_{-1}$ substitution (Foit and Rosenberg 1977; Henry and Dutrow 1996), which manifests in the variation of the Fe/(Fe+Mg) ratio, shows a slight dependence on the *X*-site occupancy. The *X*-site vacancy increases in the Fe-dominant compositions, Ca is more common in the most Mg-rich tourmaline (Fig. 6). The enrichment in Al is most likely produced by a combination of $Al\square(Mg,Fe)_{-1}Na_{-1}$ and $AlO(Mg,Fe)_{-1}(OH)_{-1}$ substitution (Foit and Rosenberg 1977; Henry and Dutrow 1996). Aluminum substitutes for Mg in the first substitution preferentially, as suggested by the weak negative correlation of Mg and *X*-site vacancy ($r = -0.54$, $r^2 = 0.30$), while Fe has no significant correlation to *X*-site vacancy, but there is some positive affinity ($r = 0.22$, $r^2 = 0.05$) (Figs S2a, b). However, there is no preference for the second substitution; both Mg and Fe have no correlations with *r* around –0.20 and r^2 below 0.05 (Fig S2c, d). Consequently, the first substitution results only in the foitite composition, while the second produces both oxy-schorl and oxy-dravite. Similarly, F shows no significant preference for either Mg or Fe, although there is a very slight indication of positive affinity to Mg ($r = 0.28$, $r^2 = 0.08$) (Figs S2e, f; ESM2). As a result, fluor-dravitic and fluor-uvitic compositions are slightly more common than fluor-schorl compositions.

Calcium is incorporated into the tourmaline structure via several substitutions. Uvite substitution, $MgCaAl_{-1}Na_{-1}$, is the most common mechanism of Ca incorporation into the tourmaline structure. It is typical of low Li tourmalines (Henry and Guidotti 1985; Henry and Dutrow 1990). This substitution results in the fluor-uvite compositions in the studied samples. Another possible mechanism for substituting Ca into *X* site in low Li-tourmalines is the $MgCaOAl_{-1}\square_{-1}(OH)_{-1}$ substitution (Henry and Dutrow 1990). The simpler variation of this substitution, the $CaONa_{-1}(OH)_{-1}$ substitution, results in the magnesio-lucchesiite end member (Scribner et al. 2021) and can have an influence on Ca-rich and F-poor compositions in the studied samples. Another common Ca-substitution in tourmalines, the $^{X}Na + {}^{Y}Al = {}^{X}Ca + {}^{Y}Li$ substitution, produces liddicoatite end member (Henry and Guidotti 1985) and is unlikely in these low-Li tourmalines. There are no indications of substitution involv-

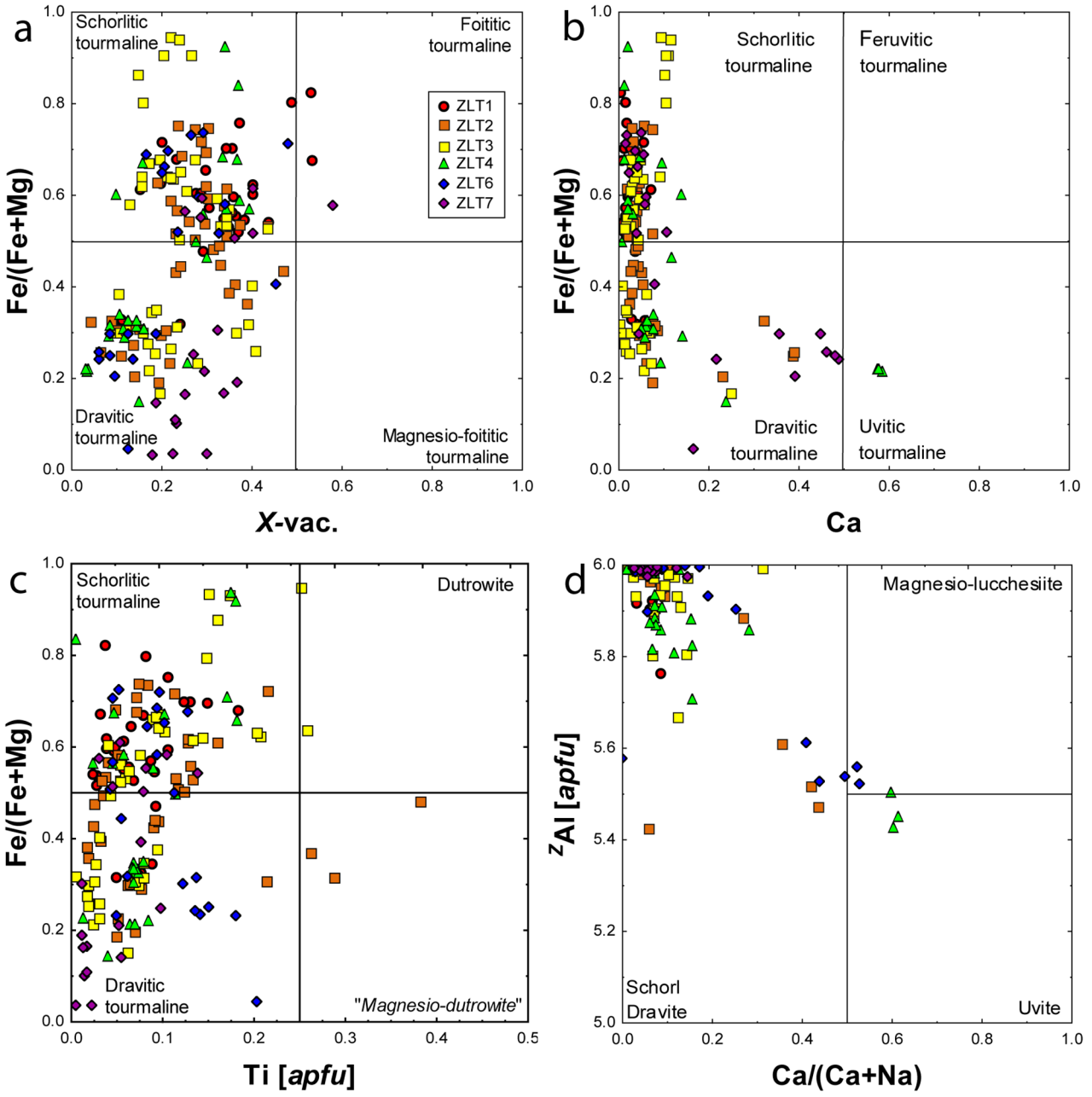

Fig. 6 Tourmaline composition diagrams. **a** – Fe/(Fe+Mg) *vs.* *X*-site vacancy. **b** – Fe/(Fe+Mg) *vs.* Ca. **c** – ^{Z}Al *vs.* Ca/(Ca+Na). **d** – Fe/(Fe+Mg) *vs.* Ti.

ing the *T* site, such as the $^{T}AlCa^{T}Si_{-1}Na_{-1}$ substitution to compensate for the charge excess at the *X* site producing the adachiite composition (Nishio-Hamane et al. 2014) in the studied samples. All Ca-rich compositions have the *T* site completely occupied by Si.

5.2. Genetic environment and evolution of tourmalinites

Tourmaline in the tourmalinites from Zlatá Idka was described as distinctly zoned, generally consisting of two zones – the older schorl (correlated with Tur I) and the younger dravite to uvite (Tur II) (Chovan et al. 2003). This was confirmed by present data, although with a greater compositional variability – Tur I shows a general trend from dravitic core to schorlitic rim. In the Al-Fe-Mg diagram (Henry and Guidotti 1985), the studied tourmalines are spread in the fields 2–7, from Li-poor granites through metapelites to Fe^{3+}-rich quartz-tourmaline rocks to low-Ca metaultramafics and Cr,V-rich metasediments (Fig. 10). This suggests a relatively great genetic variability with the influence of different factors such as the temperature, host-rock and fluid compositions on the tourmaline crystal chemistry.

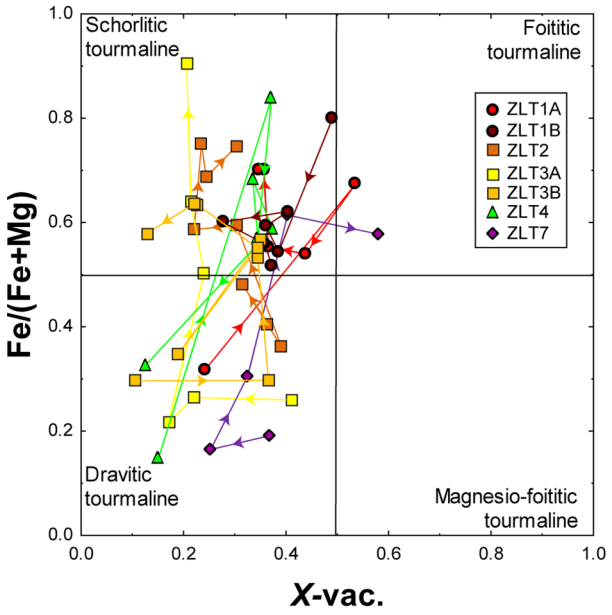

Fig. 7 Tourmaline zoning in Fe/(Fe+Mg) *vs.* *X*-site vacancy diagram.

Generally, the formation of tourmalinites can be linked to several geological processes: 1) pre-metamorphic replacement; 2) syngenetic-exhalative process; 3) submarine-hydrothermal leaching; 4) colloids and gels; 5) evaporitic processes; 6) contact metasomatism; 7) regional metasomatism (Slack 1996). These genetic processes influence the tourmaline composition and manifest in certain compositional trends. For example, tourmalinites associated with evaporites typically display the oxy-dravite–povondraite trend (Frimmel and Jiang 2001; Henry et al. 2008; Bačík et al. 2008), whereas regional metasomatic tourmalinites usually contain schorl–dravite with the Fe/(Fe+Mg) ratio resulting mostly from the geochemical properties of the host rock (Pesquera et al. 1999; Bačík et al. 2009; Houzar et al. 2014; Yücel-Öztürk et al. 2015; Arena et al. 2020; Nabelek 2021). Tourmaline from contact-metasomatic tourmalinites associated with granitic intrusions is also in the schorl–dravite trend but usually shifted towards schorl and even foitite (Smith and Yardley 1996; Bosi et al. 2018).

The compositional variability in Zlatá Idka tourmalinite indicates complex processes that likely played a role in its formation. Based on the geological setting, we can exclude some aforementioned processes (Slack 1996), such as premetamorphic replacement, syngenetic-exhalative process, colloids and gels, and evaporitic processes. Although it is not definitely excluded that these processes could take place in premetamorphic stages of the Gelnica Group rocks based on the current data, regional and contact metamorphic and metasomatic Variscan processes would have overwritten them completely. Consequently, contact or regional metasomatic processes, which overprinted older metasedimentary rocks, are most likely involved in the Zlatá Idka tourmalinite formation.

The processes resulting in tourmalinite formation can be derived from the composition and zoning of tourmalines. Previous interpretations proposed the decisive impact of metamorphic processes on the tourmalinites formation (Chovan et al. 2003). These could occur in the formation of the host rock composed of quartz, plagioclase, muscovite/illite, and chlorite. However, this interpretation goes further and assumes that during the

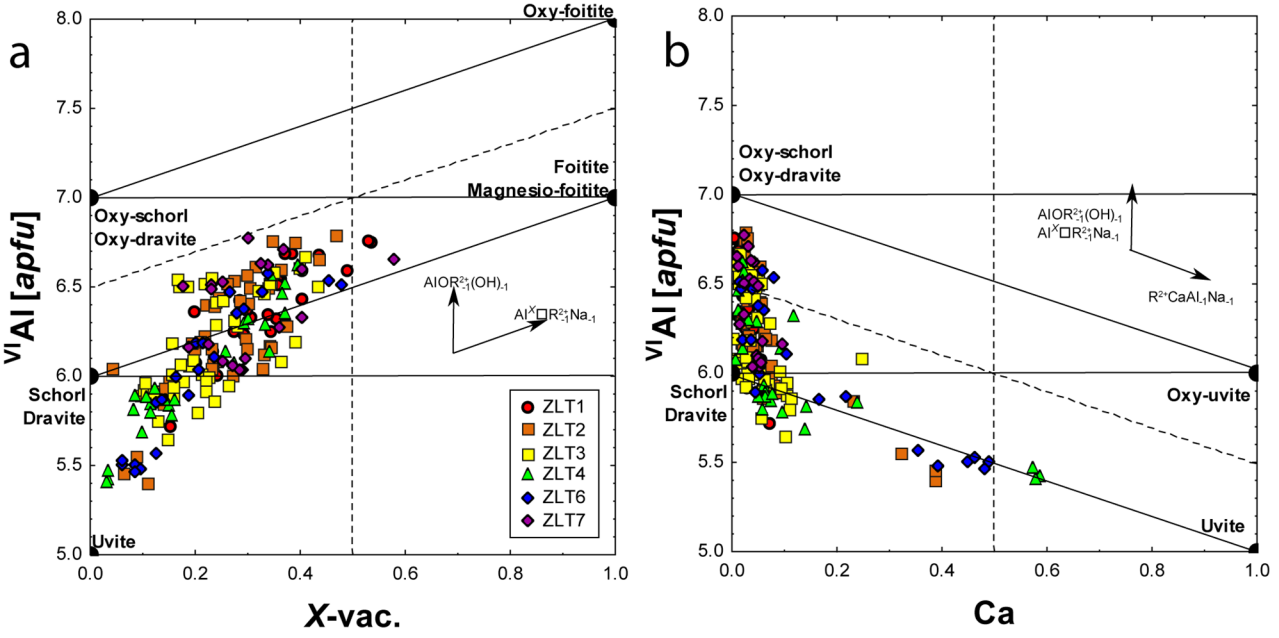

Fig. 8 Tourmaline composition. **A** – ^{VI}Al *vs.* *X*-site vacancy. **B** – ^{VI}Al *vs.* Ca.

regional metamorphic processes, the bulk of schorlitic tourmaline could form (Kobulský et al. 2000; Chovan et al. 2003). Subsequent hydrothermal processes could alter tourmaline resulting in a younger dravitic generation. The influence of the granitic intrusion was minor in this scenario (Chovan et al. 2003).

However, the influence of the granitic intrusion was likely significantly larger in the tourmaline formation. The Zlatá Idka tourmalinites occur close to Permian granite intrusion (Poproč massif) in their contact-metamorphic and metasomatic exocontact zone. The Permian granitic rocks of the Gemeric Unit show distinct S-type affinity with rare-element speciation (Li, B, F, Sn, W, Nb, Ta) and development of common accessory schorlitic tourmaline, topaz, Li-enriched micas, cassiterite, wolframite, and Nb-Ta oxide minerals (e.g., Uher and Broska 1996; Broska and Uher 2001; Kubiš et al. 2012; Broska and Kubiš 2018). The influence of late-magmatic to early post-magmatic emanations of B,F-rich fluids from these granite intrusions to adjacent metamorphic rocks could be a dominant mechanism of the Zlatá Idka tourmalinites formation. The tourmaline chemical composition and its zoning patterns, in particular, indicate the granitic source of B, F-rich fluids. The first-type tourmaline zoning in the dravite–schorl–foitite trend with an increase in the *X*-vacancies indicates a decrease in the crystallization temperature and/or decreasing salinity of coexisting fluids (Henry and Dutrow 1996; Van Hinsberg et al. 2011).

The increased F contents in tourmaline also support the influence of granite intrusion. Fluorine may originate directly from the S-type granite rich in volatile elements (Uher and Broska 1996). However, remobilization and concentration of F by overheating the host rock due to granite intrusion could also take part. However, the principal influence of metamorphic processes on the F mobilization and its concentration in tourmaline is unlikely. In metamorphic conditions, F is typically concentrated in tourmaline at a higher metamorphic grade (Henry and Dutrow 1996) which was not attained in the Gelnica Group with P–T conditions estimated between 350 and 450 °C at 3–5 kbar (Faryad 1995). Moreover, significant accumulations of tourmaline, such as Zlatá Idka tourmalinite, are not characteristic of high-grade metamorphic conditions except for premetamorphic stratiform tourmalinites remobilized during deformation and metamorphosis (Slack 1996). Consequently, the adjacent granite intrusion seems to be the most likely source of F.

The significant changes and oscillations of Tur I zoning also suggest the influence of contact metasomatic and hydrothermal processes associated with the granite intrusion in an unstable fluid regime. Granite intrusion was probably a source of heat and light elements

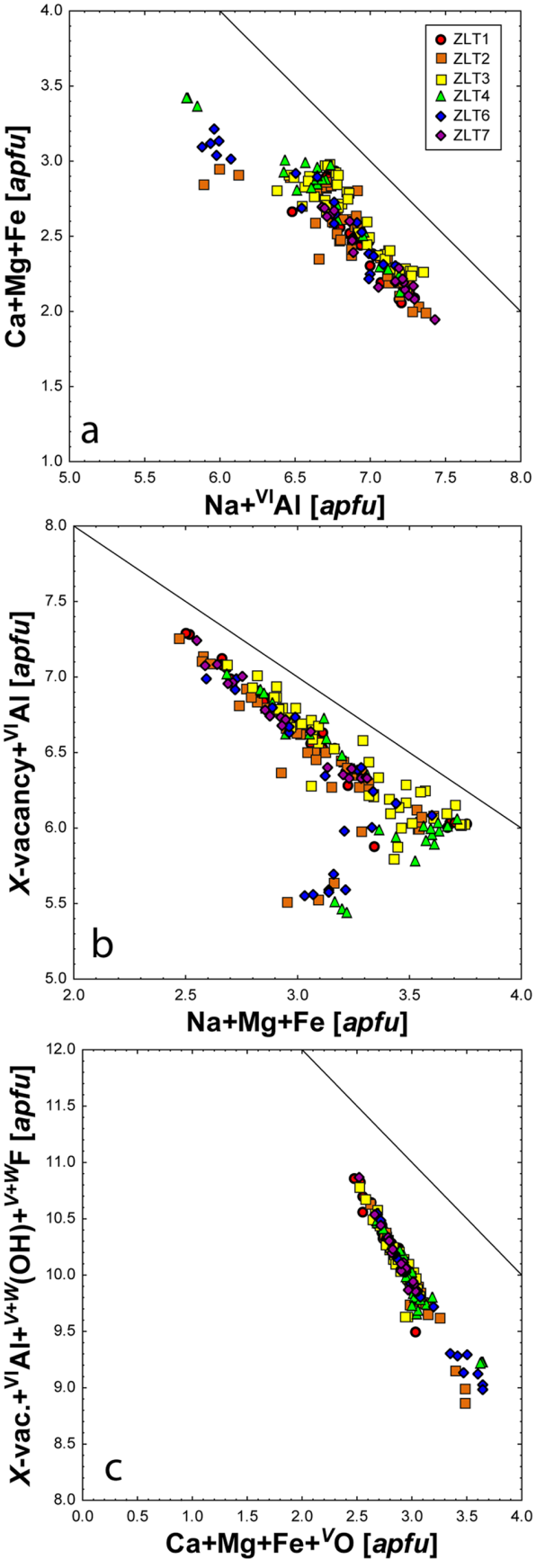

Fig. 9 Substitution diagrams of studied tourmalines. **A** – (Mg,Fe) $CaAl_{-1}Na_{-1}$. **B** – $Al^{X}\square(Mg,Fe)_{-1}Na_{-1}$. **C** – $Al^{X}\square(OH,F)(Mg,Fe)_{-1}Na_{-1}O_{-1}$.

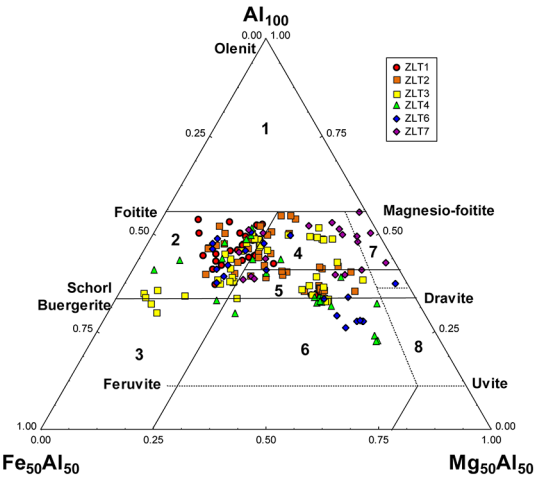

Fig. 10 Ternary Al *vs.* Fe *vs.* Mg plot (in total molecular proportions); the samples studied (points) compared with published data (fields). The fields represent distinct rock types: 1 – Li-rich granitic pegmatites and aplites; 2 – Li-poor granites and their associated pegmatites and aplites; 3 – Fe^{3+}-rich quartz-tourmaline rocks (hydrothermally altered granites); 4 – Metapelites and metapsammites coexisting with an Al-saturating phase; 5 – Metapelites and metapsammites not coexisting with an Al-saturating phase. 6 – Fe^{3+}-rich quartz-tourmaline rocks, calc-silicate rocks, and metapelites; 7 – Low-Ca metaultramafics and Cr,V-rich metasediments; 8 – Metacarbonates and meta-pyroxenites (Henry and Guidotti 1985).

(such as B and F) for extensive tourmaline formation in metamorphic volcano-sedimentary host rocks of the Gelnica group. The change in composition could result from different processes which controlled the tourmaline composition, especially granite and host-rock influence (London et al. 1996; Bosi et al. 2019). Dravitic cores of Tur I could indicate metamorphic pre-intrusion origin, as suggested by Chovan et al. (2003), but more likely indicate the host-rock control over the Tur I composition in the first phase of tourmaline crystallization. Later, the control over tourmaline composition shifted to the fluids generated from the granite resulting in the crystallization of schorl to foitite. The source of boron could be in granite intrusion, although some minor contribution from the host rock should also be expected.

In the second phase, Tur II formed on the crystal rims in some samples. This Tur II generation could also be connected to hydrothermal fluid mobilization during Alpine metamorphism (Hurai et al. 2008). However, Tur II was observed only in two samples, suggesting that the impact of fluids forming Tur II was spatially limited. Therefore, we assume that the local influence of fluids generating Tur II is more consistent with fluids derived from granite. Therefore, the chemical composition of tourmaline (Fe/Mg and Ca/Na ratio) was likely dominantly controlled by the host rock, which was partly altered by fluids. This is supported by an intriguing correlation of Ca and Ti content in the Ca-rich zones of ZLT-2 and ZLT-6 samples. This dependence has already been observed in metasomatic tourmaline on Elba Island, Italy (Dini et al. 2008), at various localities on the margins of the Leinster Granite, Ireland (Gallagher and Kennan 1992), tourmalinites from Velké Žernoseky, Czech Republic (Houzar et al. 2014) and the Black Hills, South Dakota, USA (Nabelek 2021). The mutual enrichment in both elements indicates the later mobilization and inheritance of Ca from plagioclase and Ti from biotite in the host rock (Houzar et al. 2014; Nabelek 2021). However, the exact determination of the tourmaline formation processes at this locality would require further inquiries, especially isotopic and trace-elements study of tourmaline and their host rocks.

6. Conclusions

Tourmaline in tourmalinites from Zlatá Idka displays large compositional variability with (1) alkali tourmalines schorl, dravite, fluor-schorl, fluor-dravite, oxy-schorl, oxy-dravite and "magnesio-dutrowite" (Mg-dominant analog of dutrowite); (2) calcic tourmalines fluor-uvite and magnesio-lucchesiite; (3) *X*-site vacant tourmaline foitite.

Tourmalines in all samples generally have Mg-dominant cores and Fe-dominant rims with oscillatory zoning (Tur I). Moreover, the Mg-dominant and Ca-enriched Tur II occur in ZLT-4 and ZLT-6 samples, which replaces Tur I.

The crystal chemistry of tourmaline is influenced by several substitutional mechanisms: $Mg(Fe)_{-1}$, $Al\square(Mg,Fe)_{-1}Na_{-1}$, $AlO(Mg,Fe)_{-1}(OH)_{-1}$ $(Mg,Fe)CaAl_{-1}Na_{-1}$, $MgCaOAl_{-1}\square_{-1}(OH)_{-1}$, $Ti_{0.5}O(Fe,Mg)_{-0.5}(OH)_{-1}$ and $TiMg(Al)_{-2}$ substitutions.

Tourmalinites were most likely produced by the regional or contact metasomatic processes, probably influenced by the intrusion of Permian granitic Poproč massif, as evidenced mostly by enrichment in F. However, the control of tourmaline crystallization and chemical composition varied between the intrusion and host rock. The youngest Ca-rich rims probably resulted from a later metasomatic process connected with the alteration of host-rock minerals.

Acknowledgments: We thank Patrik Konečný, Viera Kolárová, and Ivan Holický for assistance during the EMPA study. We also thank Ferdinando Bosi for editorial handling and Emily Scribner and Darrell J. Henry for their detailed reviews, which improved the quality of our work. This work was supported by the Slovak Research and Development Agency under Contract no. APVV-18-0065 and APVV-19-0065.

Electronic supplementary material. Supplementary diagrams comparing selected site occupations (Fe, Mg, Al, *X*-site vacancy proportion, ^{V+W}O and ^{W}F) are available

online on the Journal website (*http://dx.doi.org/10.3190/jgeosci.350*).

References

Arena KR, Hartmann LA, Lana C, Queiroga GN, Castro MP (2020) Geochemistry and ^{11}B evolution of tourmaline from tourmalinite as a record of oceanic crust in the Tonian Ibaré ophiolite, southern Brasiliano Orogen. An Acad Bras Ciênc 92: e20180193

Bačík P, Uher P (2007) Tourmaline group minerals from redeposited tourmalinites in Lower Triassic Quartzites, Tatric Unit, Western Carpathians. Miner Slovaca 29: 185–196

Bačík P, Uher P, Sýkora M, Lipka J (2008) Low-Al tourmalines of the schorl–dravite – povondraite series in redeposited tourmalinites from the Western Carpathians, Slovakia. Canad Mineral 46: 1117–1129

Bačík P, Pršek J, Lipka J (2009) Mineralogical research of the tourmaline-rich rocks in the metamorphosed volcanosedimentary rocks of the Jánov Grúň Complex in the Bacúch area (Veporic Superunit, Western Carpathians). Miner Slovaca 41: 433–444

Bačík P, Cempírek J, Uher P, Novák M, Ozdín D, Filip J, Škoda R, Breiter K, Klementová M, Ďuda R, Groat LA (2013) Oxy-schorl, $Na(Fe^{2+}{}_2Al)Al_6Si_6O_{18}(BO_3)_3(OH)_3O$, a new mineral from Zlatá Idka, Slovak Republic and Přibyslavice, Czech Republic. Amer Miner 98: 485–492

Bačík P, Dikej J, Fridrichová J, Miglierini M, Števko M (2017) Chemical composition and evolution of tourmaline-supergroup minerals from the Sb hydrothermal veins in Rožňava area, Western Carpathians, Slovakia. Mineral Petrol 111: 609–624

Bačík P, Uher P, Dikej J, Puškelová Ľ (2018) Tourmalines from the siderite–quartz–sulphide hydrothermal veins, Gemeric unit, Western Carpathians, Slovakia: crystal chemistry and evolution. Mineral Petrol 112: 45–63

Bajaník Š, Vozárová A, Hanzel V, Ivanička J, Mello J, Pristáš J, Reichwalder P, Snopko L, Vozár J (1983) Explanation to geological map of the Slovenské rudohorie Mts., eastern part. Dionýz Štúr Geological Institute, Bratislava, pp 1–223

Behr HJ, Ahrendt H, Martin H, Porada H, Rohrs J, Weber K (1983) Sedimentology and mineralogy of Upper Proterozoic playa-lake deposits in the Damara Orogen. In: Martin H, Eder FW (eds) Intracontinental fold belts. Springer Berlin Heidelberg, Berlin, Heidelberg, pp 577–610

Biagioni C, Bosi F, Mauro D, Skogby H, Dini A, Zaccarini F (2020) Dutrowite, IMA 2019-082. CNMNC Newsletter No. 53. Mineral Mag 84: 159–163

Bosi F, Naitza S, Skogby H, Secchi F, Conte AM, Cuccuru S, Hålenius U, De La Rosa N, Kristiansson P, Charlotta Nilsson EJ, Ros L, Andreozzi GB (2018) Late magmatic controls on the origin of schorlitic and foititic tourmalines from late-Variscan peraluminous granites of the Arbus pluton (SW Sardinia, Italy): Crystal-chemical study and petrological constraints. Lithos 308–309: 395–411

Bosi F, Naitza S, Secchi F, Conte AM, Cuccuru S, Andreozzi GB, Skogby H, Hålenius U (2019) Petrogenetic controls on the origin of tourmalinite veins from Mandrolisai igneous massif (central Sardinia, Italy): Insights from tourmaline crystal chemistry. Lithos 342–343: 333–344

Broska I, Kubiš M (2018) Accessory minerals and evolution of tin-bearing S-type granites in the western segment of the Gemeric Unit (Western Carpathians). Geol Carpath 69: 483–497

Broska I, Uher P (2001) Whole-rock chemistry and genetic typology of the West-Carpathian Variscan granites. Geol Carpath 52: 79–90

Chovan M, Moravanský D, Ozdín D, Pršek J (2003) Tourmalines – Zlatá Idka, mineralogical report. Unpublished MS, Department of Mineralogy and Petrology, Comenius University

Chown EH (1987) Tourmalinites in the Aphebian Mistassini group, Quebec. Can J Earth Sci 24: 826–830

Dini A, Mazzarini F, Musumeci G, Rocchi S (2008) Multiple hydro-fracturing by boron-rich fluids in the Late Miocene contact aureole of eastern Elba Island (Tuscany, Italy). Terra Nova 20: 318–326

Faryad SW (1995) Constraint of P-T conditions of metamorphic complexes in the Gemericum. Miner Slovaca 27: 9–19

Foit FF, Rosenberg PE (1977) Coupled substitutions in the tourmaline group. Contrib Mineral Petrol 62: 109–127

Frimmel HE, Jiang SY (2001) Marine evaporites from an oceanic island in the Neoproterozoic Adamastor ocean. Precambr Res 105: 57–71

Gallagher V, Kennan PS (1992) Tourmaline on the margin of the Leinster Granite, southeast Ireland: petrogenetic implications. Irish J Earth Sci 11: 131–150

Henry DJ, Dutrow BL (1990) Ca substitution in Li-poor aluminous tourmaline. Canad Mineral 28: 111–124

Henry DJ, Dutrow BL (1996) Metamorphic Tourmaline and Its Petrologic Applications. Rev Mineral Geochem 33: 503–557

Henry DJ, Guidotti CV (1985) Tourmaline as a petrogenetic indicator mineral: an example from the staurolite-grade metapelites of NW Maine. Amer Miner 70: 1–15

Henry DJ, Sun H, Slack JF, Dutrow BL (2008) Tourmaline in meta-evaporites and highly magnesian rocks: perspectives from Namibian tourmalinites. Eur J Mineral 20: 889–904

Houzar S, Cempírek J, Toman J, Hrazdil V, Filip J, Radoň M (2014) Turmalinit z Velkých Žernosek (Opa-

renské krystalinikum, severní Čechy). Bull mineral-petrolog Odd Nar Muz (Praha) 22: 15–24

Hurai V, Lexa O, Schulmann K, Montigny R, Prochaska W, Frank W, Konečný P, Kráľ J, Thomas R, Chovan M (2008) Mobilization of ore fluids during Alpine metamorphism: Evidence from hydrothermal veins in the Variscan basement of Western Carpathians, Slovakia. Geofluids 8: 181–207

Klimko T, Chovan M, Huraiová M (2009) Hydrothermal mineralization of stibnite veins in the Spiš-Gemer Ore Mts. Miner Slovaca 41: 115–132

Kobulský J, Kovaničová L, Repčiak M (2000) Zlatá Idka - tourmalinites. Final report. Manuscript, State Geological Institute of Dionýz Štúr, Bratislava, pp 1–97

Kubiš M, Broska I, Kubiš M, Broska I (2012) The granite system near Betliar village (Gemeric Superunit, Western Carpathians): evolution of a composite silicic reservoir. J Geosci 55: 131–148

London D, Morgan GBV, Wolf MB (1996) Boron in granitic rocks and their contact aureoles. Rev Mineral Geochem 33: 299–330

Mišík M, Jablonský J (2000) Lower Triassic quartzites of the Western Carpathians: source of clastics, transport directions. Geol Carpath 51: 251–264

Nabelek PI (2021) Formation of metasomatic tourmalinites in reduced schists during the Black Hills Orogeny, South Dakota. Amer Miner 106: 282–289

Navesňák D, Tabák J (1994) Industrial and unconventional raw materials, final report. State Geological Institute of Dionýz Štúr, Bratislava, pp 1–135

Nicholson PM (1980) geology and economic significance of the Golden Dyke dome, Northern Territory. In: Ferguson J, Goleby A (eds) Uranium in the Pine Creek Geosyncline. Int'l Atomic Energy Agency, Vienna, pp 319–334

Nishio-Hamane D, Minakawa T, Yamaura JI, Oyama T, Ohnishi M, Shimobayashi N (2014) Adachiite, a Si-poor member of the tourmaline supergroup from the Kiura mine, Oita Prefecture, Japan. J Mineral Petrol Sci 109: 74–78

Peng QM, Palmer MR (1995) The Palaeoproterozoic boron deposits in eastern Liaoning, China: a metamorphosed evaporite. Precambr Res 72: 185–197

Pesquera A, Torres-Ruiz J, Gil-Crespo PP, Velilla N (1999) Chemistry and genetic implications of tourmaline and Li-F-Cs micas from the Valdeflores area (Caceres, Spain). Amer Miner 84: 55–69

Scribner ED, Cempírek J, Groat LA, James Evans R, Biagioni C, Bosi F, Dini A, Hålenius U, Orlandi P, Pasero M (2021) Magnesio-lucchesiite, $CaMg_3Al_6(Si_6O_{18})(BO_3)_3(OH)_3O$, a new species of the tourmaline supergroup. Amer Miner 106: 862–871

Slack JF (1982) Tourmaline in Appalachian–Caledonian massive sulphide deposits and its exploration significance. Trans Inst Min Metall B: Appl Earth Sci 91(B): B81–B89

Slack JF (1996) Tourmaline associations with hydrothermal ore deposits. Rev Mineral Geochem 33: 558–643

Slack JF, Palmer MR, Stevens BPPJ, Barnes RG (1993) Origin and significance of tourmaline-rich rocks in the Broken Hill district, Australia. Econ Geol 88: 505–541

Smith MP, Yardley BWD (1996) The boron isotopic composition of tourmaline as a guide to fluid processes in the southwestern England orefield: An ion microprobe study. Geochim Cosmochim Acta 60: 1415–1427

Uher P, Broska I (1996) Post-orogenic Permian granitic rocks in the Western Carpathian–Pannonian area: Geochemistry, mineralogy and evolution. Geol Carpath 47:311–321

Van Hinsberg VJ, Henry DJ, Marschall HR (2011) Tourmaline: An ideal indicator of its host environment. Canad Mineral 49: 1–16

Yücel-Öztürk Y, Helvaci C, Palmer MR, Ersoy EY, Freslon N (2015) Origin and significance of tourmalinites and tourmaline-bearing rocks of Menderes Massif, western Anatolia, Turkey. Lithos 218–219: 22–36

Zhang JS, Passchier CW, Slack JF, Fliervoet TF, De Boorder H (1994) Cryptocrystalline Permian tourmalinites of possible metasomatic origin in the Orobic Alps, northern Italy. Econ Geol 89: 391–396

Geological map of Slovakia M 1 : 50 000 [online]. http://apl.geology.sk/gm50js. Accessed 17 Jul 2020